EEG Peak Detection in Cognitive Conflict Processing Using Summit Navigator and Clustering-Based Ranking

Tran Hiep Dinh, *Member, IEEE*, Avinash Kumar Singh, *Member, IEEE*, Nguyen Linh Trung, *Senior Member, IEEE*, Diep N. Nguyen, *Senior Member, IEEE*, and Chin-Teng Lin, *Fellow, IEEE*

***Abstract*— Correct detection of peaks in electroencephalogram (EEG) signals is of essence due to the significant correlation of those potentials with cognitive performance and disorders. This paper proposes a novel and non-parametric approach to detect prediction error negativity (PEN) in cognitive conflict processing. The PEN candidates are first located from the input signal via an adaptation of a recent effective method for local maxima extraction, processed in a multi-scale manner. The found candidates are then fused and ranked based on their shape and location-based features. False positives caused by candidates' magnitude are eliminated by rotating the sorted candidate list where the one with the second-best ranking score will be identified as PEN. The EEG data collected from a 3D object selection task have been used to verify the efficacy of the proposed approach. Compared with the state-of-the-art peak detection techniques, the proposed method shows an improvement of at least 2.67% in accuracy and 6.27% in sensitivity while requires only about 4 ms to process an epoch. The accuracy and computational efficiency of the proposed technique in the detection of PEN in cognitive conflict processing would lead to promising applications in performance improvement of brain-computer interfaces (BCIs).**

***Index Terms*— Summit navigator, peak detection, spike detection, electroencephalogram (EEG), cognitive conflict, prediction error negativity (PEN), error-related positive potential (Pe), clustering.**

I. Introduction

COGNITIVE conflict is the reaction of the human brain when observing a mismatch (error) between a prediction of an on-going action and its actual results. This process can be interpreted via analyzing the event-related potential (ERP) in electroencephalogram (EEG) [1] and has shown great application potentials, such as intuitiveness estimation in physical human-robot collaboration [2] and impact evaluation of visual styles in virtual reality [3].

Choice reaction tasks were first designed in [4]–[7] to study error processing. Notably, the presence of two components, namely the error-related negativity (ERN or Ne) [8] and the error-related positive potential (Pe) [9], have been observed when cognitive conflict occurs. Consequently, various studies on error-related potentials have been conducted to demonstrate the appearance of cognitive conflict in different scenarios, such as during interactions with a simulated BCI [10], or via computer tracking tasks [11].

Recent works [3], [12], [13] have evaluated that the prediction error negativity (PEN) is elicited due to the recognition of a discrepancy between the awareness and the prediction of 3D environment changes. This negativity can be categorized as a family of ERN. An illustration of PEN and other event-related potentials are demonstrated in Figure 1 where positive potentials P1, P2, P3 peak respectively at around 100, 200, and 300 ms, and negative potentials N1, PEN, N4 peak respectively at around 100, 200, and 400 ms. It is worth noting that the amplitudes and locations of the ERP components are of great importance to analyze the difference between erroneous and correct responses in abnormal action monitoring, where patients with anxiety, depression, or substance abuse are reported with increased ERNs [14]. Hence, an effective and robust automatic peak detection algorithm would lead to not

Manuscript received August 23, 2021; revised January 10, 2022 and April 6, 2022; accepted May 17, 2022. Date of publication May 30, 2022; date of current version June 14, 2022. This research has been done under the research project QG.22.63 "Development of an EEG peak detection algorithm in cognitive conflict processing and its application in communication assistance systems" of Vietnam Nation University (VNU) Hanoi. This work is also supported in part by the Joint Technology and Innovation Research Centre (JTIRC), a partnership between the University of Technology Sydney and the VNU University of Engineering and Technology, and in part by the Australian Research Council (ARC) under Grant DP210101093 and Grant DP220100803. *(Corresponding author: Tran Hiep Dinh.)*

This work involved human subjects or animals in its research. Approval of all ethical and experimental procedures and protocols was granted by the Ethics Committees of the University of Technology Sydney, Australia.

Tran Hiep Dinh is with JTIRC, University of Engineering and Technology, Vietnam National University, Cau Giay, Hanoi 100000, Vietnam (e-mail: tranhiep.dinh@vnu.edu.vn).

Avinash Kumar Singh and Chin-Teng Lin are with the Faculty of Engineering and Information Technology, School of Computer Science, Australian Artificial Intelligence Institute, University of Technology Sydney, Sydney, Ultimo, NSW 2007, Australia (e-mail: avinash.singh@uts.edu.au; chin-teng.lin@uts.edu.au).

Nguyen Linh Trung is with the Advanced Institute of Engineering and Technology (AVITECH), University of Engineering and Technology, Vietnam National University, Cau Giay, Hanoi 100000, Vietnam (e-mail: linhtrung@vnu.edu.vn).

Diep N. Nguyen is with the Faculty of Engineering and Information Technology, School of Electrical and Data Engineering, University of Technology Sydney, Sydney, Ultimo, NSW 2007, Australia (e-mail: diep.nguyen@uts.edu.au).

Digital Object Identifier 10.1109/TNSRE.2022.3179255

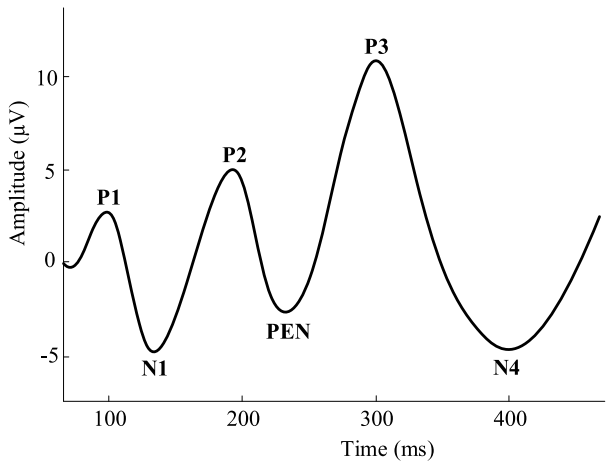

Fig. 1. Illustration of PEN and other potentials in an epoch.

only an accurate detection of those ERP components but also a correct diagnosis of those disorders.

Among the most popular approaches [15], [16] when dealing with the EEG spike detection problem, the window analysis techniques are widely used due to their easy implementation and simplicity. The ERP amplitude is calculated as the mean of the local extrema of the time window of interest and its nearest neighbors [3], [6], [12], [13], while the latency is taken from that of the local extrema. Despite the straightforwardness, this approach might miss the true peak when multiple candidates appear in the interested time window.

To tackle this challenge, particularly in cognitive conflict, and generally in EEG signal processing, various automatic detection algorithms have been proposed, including morphology [17]–[19], rule-based [20]–[22] approaches and artificial intelligence systems [23]–[26]. A signal separation technique was introduced in [17], where spike portions can be extracted from the background EEG using morphological filters. An improved version is then proposed in [18], where an average weight has been added to the morphological operation design for elimination of statistical deflection of amplitude, and the construction of the structuring elements are optimized. Although this type of method was verified in simulated data and the intracranial EEG recordings [19], its effectiveness is sensitive to the design of the structuring element. In the rule-based systems [20]–[22], the characteristics of the spikes, such as shape, slope, width are employed to generate patterns, where the similarity between a concerned time window and the generated pattern is calculated to determine if a spike exists. Due to the intra-subject variability [27] and artifacts [28], these approaches might be vulnerable to features that do not match the pre-defined patterns.

With the recent development in artificial intelligence, many machine and deep learning-based approaches have been proposed, where peak features are extracted from sampled time windows for training and testing a model. For machine learning techniques, such as Ant K-Means Clustering [23] and Support Vector Machines [24], feature engineering is an essential yet tedious process that has a vital effect on the capability of the system. This process is eased in DL methods [25], [26], [29], as features are automatically generated in multilevel layers of a convolutional neural network. Although the obtained results from those methods are promising, they require a large amount of correctly labeled data samples.

It can be seen that existing peak detection algorithms are either based on conventional methods with a priori knowledge about the data and user-input parameters or DL algorithms with a dataset of high quality and large training samples. To deal with the parameter dependence in the former, we propose an automatic peak detection approach and apply it on PEN determination in cognitive conflict processing. An adaptation of a recent effective technique for local extrema extraction, the Summit Navigator (SN) [30], is developed for the calculation of PEN candidates. A ranking scheme based on clustering is proposed to select the most outlying candidate from the determined ones, mimicking neurology experts' decision in PEN selection. The proposed approach is then validated on the dataset obtained from a 3D object selection task [3]. The major contributions of this work are summarized as follows:

- The adaptation of a local maxima extraction algorithm for image segmentation to EEG signal processing, the effectiveness of which have been verified through extensive experiments.
- An innovative ranking scheme based on clustering combining with the adapted SN for PEN detection in cognitive conflict processing.
- The leverage of the non-parametric feature to minimize the dependence on user interference and increase the adaptability of the proposed approach to the variability in EEG signals.

The rest of the paper is as follows. The proposed method using SN and Clustering-based Ranking (CR) is described in Section II. Experimental results and discussion are respectively presented in Sections III and IV. Finally, the conclusion is drawn in Section V.

II. Methodology

A. Multi-Scale Peak Searching

Due to the difference in subjects' behavior and experimental paradigms, PENs have been observed and extracted in similar but not identical time frames. For instance, it has been pointed out in [31] that a PEN is detected from 100 to 200 ms when variations in the motor output and visual input are noticed. On the other hand, the PEN is discovered around 50-150 ms in a virtual object selection task [12], or 100-300 ms in a haptic immersion study [32]. While a correct detection of PENs is of importance for further analysis, the selection process is quite straightforward: the PEN can be extracted from the concerned time window as its minimum [32], or as the mean of the minimum and its nearest neighbor [12]. Despite its simplicity and effectiveness, the following concerns have not been addressed in this type of approach: (i) the requirement of a pre-defined time window, and (ii) the appearance of multi-minimums in the concerned range.

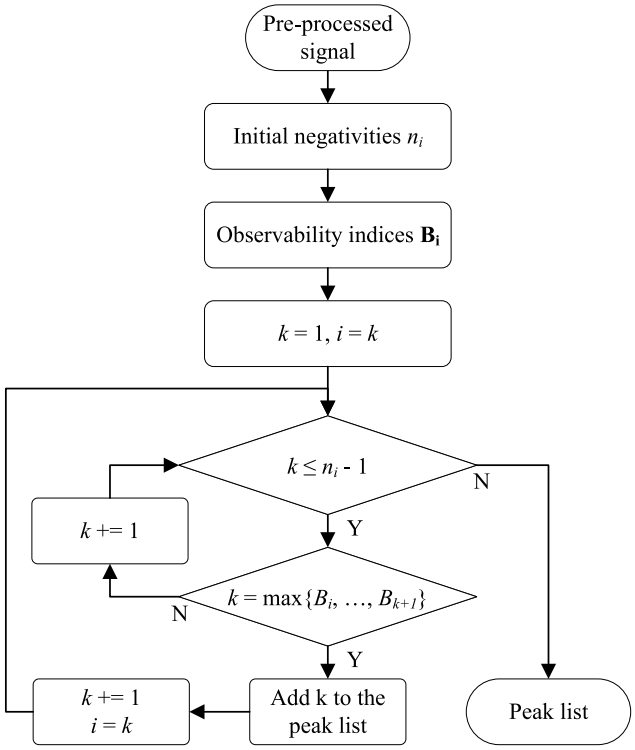

Fig. 2. Pipeline of the SN-based peak determination.

Here, we propose to extract peaks in the signal in a multi-scale manner, covering the time windows where the appearance of PENs have been reported. Specifically, PENs will be analyzed in multiple time windows $[t_{s_i}, t_{e_i}]$, where $\vec{t_s} = \{50, 75, 100\}$, and $\vec{t_e} = \{250, 225, 200\}$. A novel peak detection technique based on SN is also developed to deal with the multi-minimums in each time window. SN is initially proposed in [30] for image segmentation purposes by searching for peaks and valleys from the histogram of the input image. The technique consists of two stages: peak searching and peak merging. While the focus of the first stage is to detect dominant peaks from the signal, that of the second stage is to remove the false positives from the searching phase based on a uni-modal hypothesis. Although the first stage is non-parametric, a fixed threshold is required in the second stage for the removal of false positives. Since the goal of this study is an automatic peak detection approach where no input is required, only the first part of SN is inherited for PEN candidate detection, and a ranking scheme is then proposed to select the most appropriate PEN. The PEN candidate detection process in each time window is described as follows.

Let y_i be the pre-processed signal in the i-th time window W_i with n_i initial negativities stored in $\vec{T}_{n_i}$. Here, a data point is defined as an initial negativity if it is more negative or equal to that of its nearest neighbors. A set $\vec{P}_i$ of dominant negativities is calculated based on two indicators, namely the offset distance and observability index as described in [30]. For each initial negativity $t^{(j)}$, $2 \leq j \leq n_i$, possible observing locations are formulated as:

$$\vec{L}^{(j)} = t^{(j)}\vec{e}_{j-1} - (y^{(j)}\vec{e}_{j-1} \circ \vec{\Delta}t^{(j)}) \oslash \vec{\Delta}y^{(j)}, \tag{1}$$

where $\vec{e}_{n_i-1}$ is the $(j-1)$-element vector of all ones. The differences between the initial negativity $t^{(j)}$ and its previous neighbors in terms of location and amplitude are stored respectively in two vectors $\vec{\Delta}t^{(j)}$, $\vec{\Delta}y^{(j)}$, which are defined as

$$\vec{\Delta}t^{(j)} = t^{(j)}\vec{e}_{j-1} - \left[t^{(1)}\ t^{(2)}\ \ldots\ t^{(j-1)}\right], \tag{2}$$

$$\vec{\Delta}y^{(j)} = y^{(j)}\vec{e}_{j-1} - \left[y^{(1)}\ y^{(2)}\ \ldots\ y^{(j-1)}\right], \tag{3}$$

in which $\circ$ and $\oslash$ are respectively the element-wise multiplication and division operators, with any zero element of $\vec{\Delta}y_j$ being substituted by some small number ϵ. The best observing location, L^*, is then given by:

$$L^* = \min_{n_i}\{\min_{j} \vec{L}^{(j)}\}. \tag{4}$$

The observability indices of all negativities in W_i calculated based on L^* is then determined as:

$$\vec{B}_i = \vec{Y}_i \oslash (\vec{T}_{n_i} - \vec{L}^*_{n_i}), \tag{5}$$

where $\vec{Y}_i$ is the vector of voltage values of all elements in $\vec{T}_{n_i}$, and $\vec{L}^*$ is the n_i vector of all L^*s. Based on the indices calculated in Eq. (5), the first dominant negativity is determined at k if B_k is the maximum value among $\{B_1, B_2, \ldots, B_{k+1}\}$. Once the first dominant negativity is located, the search will be re-implemented on the remaining part of the list, starting from $k+1$ to find the next dominant one. This process runs recursively until k reaches $n_i - 1$. The n_ith negativity is also identified as dominant if its index B_{n_i} is greater than that of the neighbor ones. The found dominant negativities in W_i is then saved in $\vec{P}_i$. The pipeline of the SN-based peak determination is illustrated in Figure 2.

B. Clustering-Based Ranking (CR) for PEN Determination

The dominant peaks found in each of the three selected time windows are then fused to get a final list of PEN candidates, i.e.

$$\vec{C} = \bigcup_{i=1}^{3} \vec{P}_i. \tag{6}$$

As mentioned in [12], the PEN is followed by an error positivity (Pe) around [250, 350] ms. Hence, the distance from the PEN to the center of the window containing the Pe is an important factor to identify the most appropriate candidate. Besides, other features such as the width and amplitude of the candidates are reported as essential factor characterizing the error related potentials [10], [33]. Here, a candidate should be negative and broad enough while being located not too far from the Pe interval to be considered as PEN by a neurologist. To implement this idea, a clustering-based ranking approach for PEN determination is proposed and illustrated in Figure 3. The idea behind this approach is to rank the candidates based on their dissimilarity to the remaining ones and determine the most outlying observation as PEN, taking into account essential features required for a manual selection process.

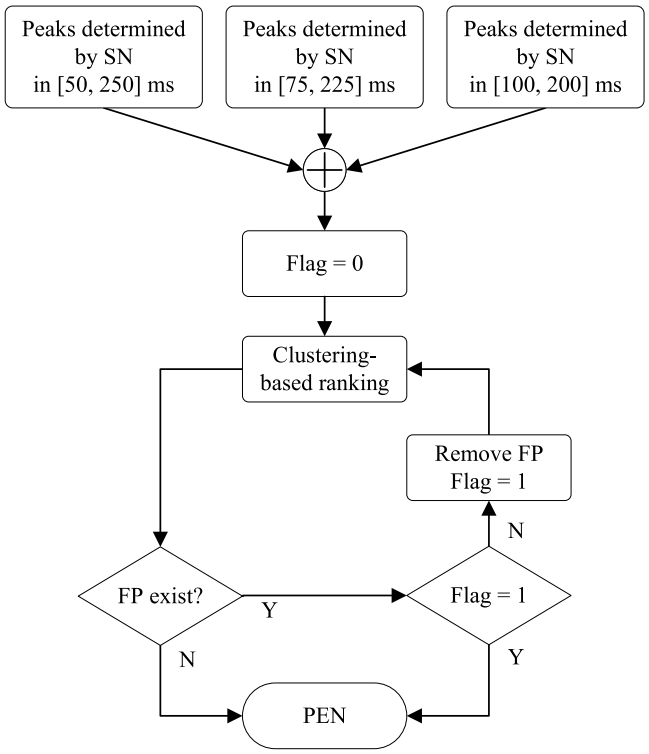

Fig. 3. Pipeline of the PEN selection approach.

Here, each candidate $c_k \in \vec{C}$ is characterized by its amplitude a_k, width w_k, and distance s_k to the [250, 350] ms and represented in the parameter space as

$$c_k = (a_k, w_k, s_k). \tag{7}$$

Let m be the number of PEN candidates determined in Eq. (6). For each candidate c_k, a cluster $\vec{C}_k$ formed by the remaining $(m-1)$ peaks in $\vec{C}$ while disregarding c_k is defined as

$$\vec{C}_k = \vec{C} \backslash \{c_k\}, \tag{8}$$

The coordinates $(a_{\mu_k}, w_{\mu_k}, s_{\mu_k})$ of the cluster center, μ_k, in the parameter space is calculated as

$$\mu_k = \frac{1}{m-1} \sum_{j \in \vec{C}_k} (a_j, w_j, s_j). \tag{9}$$

The Euclidean distance from the candidate c_k to the cluster center μ_k is then determined as

$$d_k = \sqrt{(a_k - a_{\mu_k})^2 + (w_k - w_{\mu_k})^2 + (s_k - s_{\mu_k})^2}. \tag{10}$$

Candidates in $\vec{C}$ are then ranked based on their distance d_k to the corresponding cluster center μ_k, and the one with the highest value among the set of cluster distances $\vec{D}$ is selected as PEN. Figure 4 demonstrates the processing steps of the proposed clustering-based ranking approach where 4 candidates are identified respectively at 72, 112, 148, and 232 ms (Figure 4(a)). For convenience, those candidates are denoted from 1 to 4 in Figure 4(b) according to the increasing order of their locations. Figure 4(b) also presents corresponding cluster distances, and highlights the determined PEN in red.

Algorithm 1 Clustering-Based Ranking

Input: m ▷ number of PEN candidates
Output: PEN

```
PEN ← None
maxDist ← 0
for k = 1 → m do
    Form cluster C_k as in Eq. (8)
    Calculate distance d_k as in Eq. (10)
    if d_k > maxDist then
        maxDist ← d_k
        PEN ← c_k
    end if
end for
```

This approach is, however, impacted by trials where a peak is much less negative than the remaining ones. In that case, the most insignificant peak is featured by the highest cluster distance and hence could be determined as PEN. However, candidates with the least negative amplitude are less likely to be selected by the neurology expert. To automatically disregard this most insignificant peak, the candidate with the highest cluster distance but the least amplitude is classified as a false positive. The least value of the calculated cluster distances is also assigned to this false positive so it is no longer identified as PEN. This False Positive Removal (FPR) mechanism is illustrated in Figure 5 where candidates 1, 2, 3 are respectively found at 60, 100, and 124 ms. According to the initial ranking in Figure 5(b), candidate 3 has the highest distance to the remaining one as per Eq. (10) but should not be selected as PEN due to its close to zero amplitude (represented as black in Figure 5(a)). This FP (represented as black in Figure 5 (b)) is then removed by replacing its distance by the least value among the found candidates (i.e. that of candidate 1) as illustrated in Figure 5(c). After updating the candidates' distance values, the correct PEN is detected and represented in red in Figure 5(a) and (c). The pseudo-code of the clustering-based ranking algorithm is presented Algorithm 1.

C. Dataset and Evaluation Metrics

The dataset used in this paper was obtained in [3] based on a virtual 3D object selection task. After applying a 0.5 Hz high-pass and a 50Hz low-pass finite impulse response (FIR) filters on the obtained EEG signals, a down-sampling to 500Hz is implemented for data reduction. Independent component analysis [34] is then employed for the removal of eye movement and muscle activity artifacts where the remaining independent components are projected back to selected channels for further analysis. The time window for epochs extracted from the processed signals is 200 ms prior to the event onset to 800 ms after the response. The dimension of the obtained data where cognitive conflict occurred is 12 subjects × 62 channels × 375 data points × 2375 epochs.

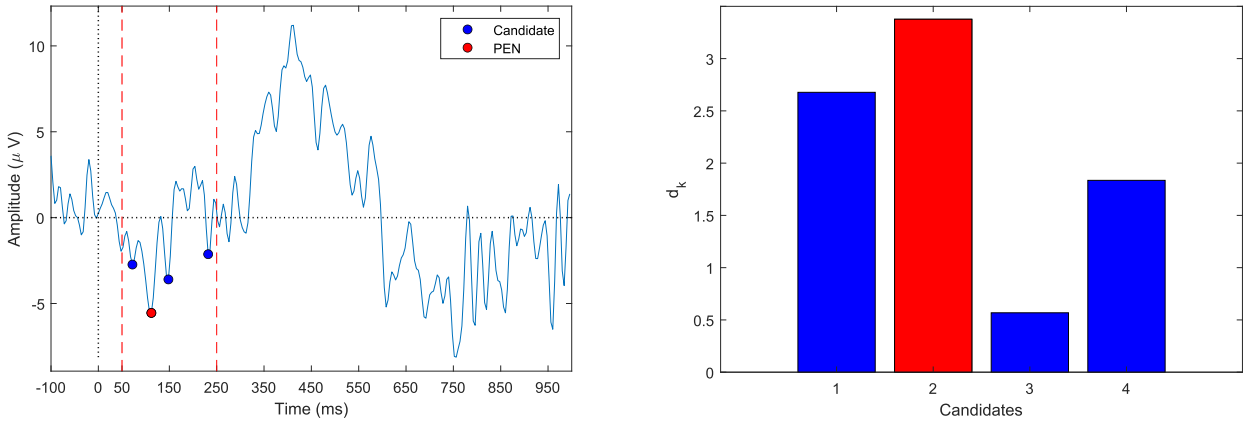

(a) (b)

Fig. 4. Demonstration of the proposed clustering-based ranking approach on an epoch with: (a) peak candidates, and (b) peak ranking.

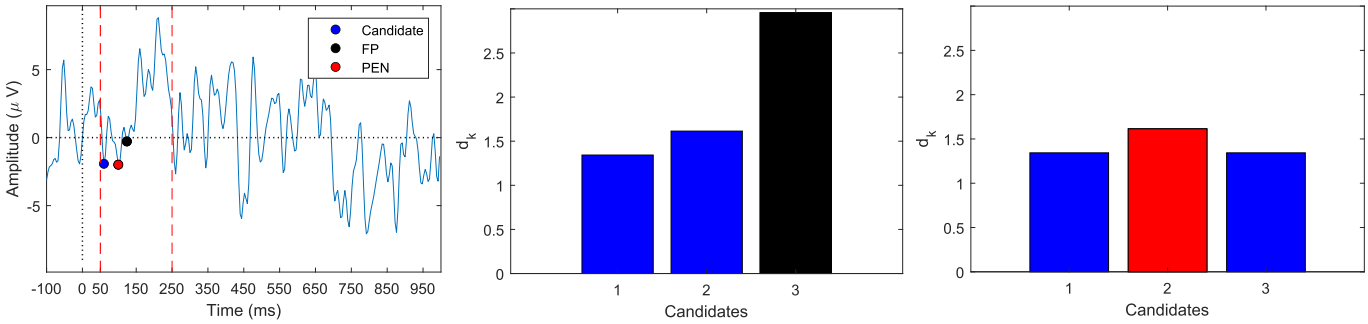

(a) (b) (c)

Fig. 5. Demonstration of the proposed FPR: (a) peak candidates, peak ranking (b) before and (c) after the removal of the false positive.

As suggested in [3], the signal at the electrode location FCz is employed to evaluate the performance of comparative algorithms in this study. The PEN location in each epoch was labeled by a neurology expert. For quantitative comparison, the sensitivity (Sen), specificity (Spe), Accuracy (Acc), and Kappa score (K) are employed and given as follows:

$$Sen = \frac{TP}{TP + FN}, \tag{11}$$

$$Spe = \frac{TN}{TN + FP}, \tag{12}$$

$$Acc = \frac{TP + TN}{N}, \tag{13}$$

$$K = \frac{Acc - P_e}{1 - P_e}. \tag{14}$$

Here, TP and TN are respectively the number of correct detection of PEN and non-PEN while the number of incorrect detection of that are respectively represented by FP and FN, and N is the total number of classifications. The Kappa score is measured as a function of the actual and the expected accuracy, Acc, and Pe, where

$$P_e = P_{pos} + P_{neg}, \tag{15}$$

$$P_{pos} = \frac{(TP + FN) \times (TP + FP)}{N^2}, \tag{16}$$

$$P_{neg} = \frac{(TN + FP) \times (TN + FN)}{N^2}. \tag{17}$$

III. Results

A. Comparative Algorithms

In this section, experiments on the dataset obtained from the study on cognitive conflict using a 3D object selection task [3] was carried out to evaluate the effectiveness of the proposed approach in cognitive conflict processing, where the following peak detection approaches are selected for comparison:

- Morphology-based Approach (MA) [19]: the peaks are extracted from the EEG signal by using a combination of two morphological filters: opening-closing and closing-opening, where a triangle structure element is selected to optimize the performance of the transform.
- Derivative-based Approach (DA) [21]: potential peaks are compared with their neighbors in a trimmed time series, where a magnitude constraint is required to select the most appropriate ones.
- Pattern Matching-based Approach (PMA) [22]: EEG peaks are defined by matching the characteristics of a trimmed time series with a pre-defined pattern where the similarity index and amplitude thresholds are adjustable thresholds for peak selection.
- Normalized Cumulative Energy Difference (NCED) [35]: EEG peaks are extracted from noisy signal based on the energy difference between a spike and a noise of the same length. The normalized cumulative energy is first

TABLE I
ACCURACY EVALUATION

Method	Sen	Spe	Acc	K
MA [19]	0.8851	0.9690	0.9512	0.8541
DA [21]	0.8682	0.9645	0.9440	0.8327
PMA [22]	0.8720	0.9655	0.9456	0.8375
NCED [35]	0.8568	0.9614	0.9392	0.8183
AA [13]	0.8682	0.9645	0.9440	0.8327
CA	0.8973	0.9723	0.9564	0.8696
SN [30]	0.8829	0.9684	0.9503	0.8514
SNCR w/o FPR	0.8215	0.9519	0.9242	0.7734
SNCR	**0.9600**	**0.9892**	**0.9830**	**0.9492**

calculated then a cut-off threshold is applied for peak selection.

- Averaging-based Approach (AA) [13]: in this study, PEN peaks are selected as the minimum amplitude in the search window and characterized as the mean of the local minimum and its nearest neighbors.
- Commercialized Approach (CA): peaks are extracted from the signal background using the built-in function ***findpeaks*** in MATLAB R2020a.

For each epoch, data points within the interested range that are more negative than their nearest neighbors are identified as peak candidates as illustrated in Figures 4 and 5. Since the number of peaks returned by each comparative approach is different due to their specific searching mechanism, the following setting was applied for a fair comparison. For a correct detection of each participated algorithm, its number of TN was $n-1$ and $FP = FN = 0$, where n was the number of found candidates in the concerned epoch. For an incorrect detection, TP, TN was assigned respectively as 0 and $n-2$, where $FP = FN = 1$. For comparative approaches that return more than one candidates (DA, AA, SN), the most negative one was identified as PEN. The experiments were executed by using MATLAB R2020a on an Intel(R) Core(TM) i5-6200U CPU @2.30 GHz with 64 bit Windows 10. The performance of comparative algorithms are reported and discussed in the next sections.

B. Results

1) Accuracy Evaluation: Performance of comparative algorithms is reported in Table III. Notably, SNCR outperforms other algorithms in terms of sensitivity, specificity, and accuracy, and Kappa score, indicating a high agreement between the expert's selection and the calculated PEN. Out of 2375 epochs, SNCR only misdetects 95 PENs from 11186 candidates. The importance of the FPR mechanism is also highlighted since a significant drop in sensitivity (−0.1385), specificity (−0.0373), and accuracy (−0.0588) occurs when FPR is removed from the proposed approach (SNCR w/o FPR). The performance of SN is also evaluated in this experiment where the threshold for the peak merging phase is selected at 0.45 as suggested in [30]. As reported in Table I, results returned by SN when the merging phase is involved is close to that of CA when searching for the most isolated candidates. Notably, when assessing the efficiency of SN with only the searching phase where the observability index (Eq. (5)) is employed as a selection criterion, performance metrics $\{Sen, Spe, Acc, K\}$ of SN have significantly dropped to $\{0.8261, 0.9531, 0.9262, 0.7792\}$. This has confirmed the advance of SNCR against the original algorithm in not only the accuracy in PEN selection but also in the automation of the process since no parameter is required.

As a commercialized approach, CA provides researchers with various options related to the magnitude or isolation level of a peak to specify the candidates to be detected. In the former group, the threshold of the absolute magnitude or the relative difference of that between a peak and its adjacent neighbors are taken into account. These mechanisms are similar to that of DA and AA and hence not reported in this section. The latter measures the isolation level of a peak by only taking into account significant candidates that are separated by at least a minimum distance and ignoring the smaller ones. When identifying the most isolated candidate as PEN, the best performance of CA, i.e. ranked second among comparative algorithms, is achieved when the minimum distance threshold is set at $0.95 \times (\max(t) - \min(t))$ where t is the timestamps of the input signal.

On the other hand, PMA and MA returns promising results in all evaluation metrics. The performance of MA is dependent on the length L of the structuring element and achieves the best in this dataset when L is set to 49. Due to the dependence of PMA on the similarity between the interested peak and the pre-defined pattern as well as the threshold required for the peak magnitude, different parameter settings have been conducted for a fair comparison. Here, a candidate k is only identified as PEN if the similarity index C_k, magnitude difference A_k, or the product $C_k \times A_k$ of those indices is the highest among the existing ones. In this experiment, the best performance of PMA is achieved and reported when the highest similarity condition is applied. The lower performance of MA and PMA compared to SNCR can be explained by the focus of the approaches on candidates with high degree of symmetry that does not really match with the variety of signals obtained.

NCED, DA and AA return acceptable results, where that of DA is adjustable by changing the threshold difference Δ between a candidate and its surrounding. The higher value Δ is assigned, the more selective the approach is, i.e. less results can be returned from the test epochs. For instance, when Δ is set to 5 or 10 μV, DA can only find peaks on 2198 or 1550 epochs, respectively. By the default setting $\Delta = (\max(y) - \min(y))/4$, where y is the input signal, DA performs well on all 2375 epochs, the results of which are reported in Table III. Since the PEN selection mechanism of DA is set to be identical to that of AA, which treats the most negative candidate more favorably, the results returned by these techniques are similar. On the other hand, a threshold is required on the first differential of the normalized cumulative energy in NCED to determine the most significant peaks. In this experiment, NCED returns its best average performance

TABLE II
COMPUTATIONAL EFFICIENCY EVALUATION

Method	PTPE (ms)	EPS
MA [19]	12.0431	83.0348
DA [21]	2.1090	474.1548
PMA [22]	2.2226	449.9256
NCED [35]	2.4532	407.6329
AA [13]	**2.0643**	**484.4367**
CA	2.7628	361.9489
SN [30]	4.2935	232.9082
SNCR w/o FPR	4.0520	246.7894
SNCR	4.0576	246.4488

if the threshold is set equal to the double of the mean value of the smoothed signal.

2) Computational Efficiency Evaluation: The proposed algorithm consists of two stages, Multi-scale Peak Searching (MPS) and Clustering-based Ranking for PEN Determination (CRPD), the average processing time per epoch (PTPE) of which is 3.8193 ms and 0.2383 ms, respectively. The computational efficiency in terms of PTPE and number of epoch per second (EPS) of the proposed and other comparative algorithms is reported in Table II. FPR, although plays an essential part in boosting the accuracy of SCR, takes only 0.0056 ms in average in processing an epoch. In a comparison with the original algorithm SN [30], SNCR is faster in terms of PTPE and has a higher EPS. Among the comparative algorithms, AA is the most computationally effective due to its simple searching mechanism while the morphology-based approach, MA, returns the least EPS. Although not being ranked as the fastest algorithm, an unoptimized version of SNCR has shown the capability of processing more than 245 epochs per second. This trait is important when implementing the algorithm on a real-time BCI system, where other stages such as pre-processing and classification are involved and data are fed from multiple channels.

C. Further Analysis

1) Number of Time Window: As discussed in Section II-A, the multi-scale searching mechanism is employed in this paper to cover the time windows where the occurrence of PENs have been reported. Besides, results of the SN-based peak determination are relied on the density and amplitude of the local data points. Hence, the width of and distance between the designed time windows should be sufficient to contain multiple peak candidates and increase the chance to detect the correct PEN. Applying a dense time window distribution on the interested range would increase the computational cost while too few time windows could lead to a mis-detection of a candidate. In practice, we have found that three windows of size 100, 150, and 200 ms work well on the analyzed data.

2) Choice of Clustering Algorithm: Since the ranking of the candidates is based on the grouping nature of the input data, the selection of the clustering algorithm is important. The desired algorithm should be effective in finding the dissimilarity in the observations and straightforward in implementation. Equally important is the number of adjustable parameters required for the selected algorithm. More tunable parameters could increase the detection accuracy but also the bias towards the training data. While such algorithms as BIRCH [36], DBSCAN [37], or CFSFDP [38] are well-known for their effectiveness, at least two parameters are required to estimate the number of cluster and the cluster density. On the other hand, only the former is needed in k-means clustering [39]. Hence, k-means clustering is selected for our approach. As described in section II.B., the candidates are ranked based on their distance to the cluster formed by the remaining ones, i.e. the number of cluster required for the k-means algorithm in each iteration is fixed at one.

TABLE III
PERFORMANCE OF SNCR USING DIFFERENT DISTANCE METRICS

Distance	Sen	Spe	Acc	K
Euclidean	**0.9600**	**0.9892**	**0.9830**	**0.9492**
Manhattan	0.9520	0.9871	0.9796	0.9391
Chebychev	0.9411	0.9841	0.9750	0.9252
Correlation	0.4905	0.8627	0.7837	0.3532
Cosine	0.4766	0.8589	0.7778	0.3356

3) Distance Metric: To evaluate the performance of the proposed SNCR using different distance metrics, Euclidean, Manhattan, Chebychev, Cosine, and Correlation distances are employed, the results of which are reported in Table III. It is significant to see that Euclidean, Manhattan, and Chebychev distances are more favorable in the proposed clustering-based ranking stage, taking into account the magnitude differences in the feature space coordinates. On the other hand, SNCR performs poorly with distances that consider the angle difference or the correlation between the feature vectors. Among the comparative measures, the Euclidean distance is selected due to the best results returned in all accuracy evaluation metrics.

IV. DISCUSSION

In the previous section, the performance of the proposed approach has been evaluated and compared with related peak detection algorithms. The out-performance of SNCR over participated algorithms stemmed from the following: (i) The clustering algorithm is designed based on neurology expert knowledge in PEN selection where the dissimilarity of a candidate to the remaining ones is highlighted by a cluster distance; (ii) the employment of SN in the peak detection and FPR in the false-positive removal process is essential to remove insignificant peaks and false PEN, respectively. With the aim of developing an automatic peak detection for cognitive conflict processing, the non-parametric feature has been emphasized in the approach. Should the FPR be processed more than once in each epoch, the performance of SNCR can be improved in some cases. However, a predefined threshold is required to specify the number of FP. The automation of the approach, in this case, can no longer be maintained.

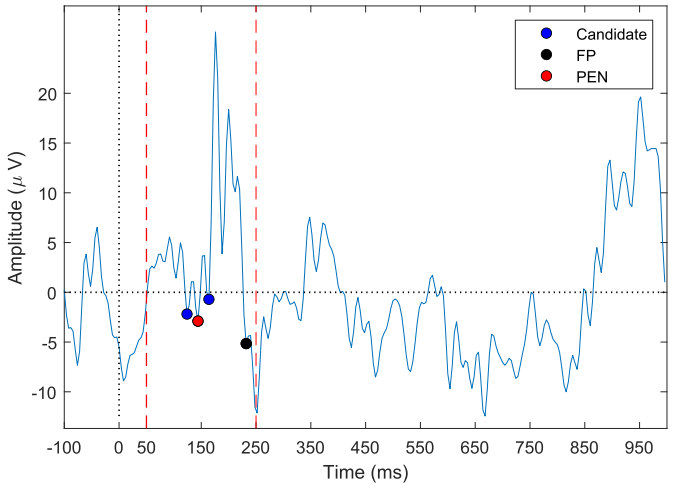

(a)

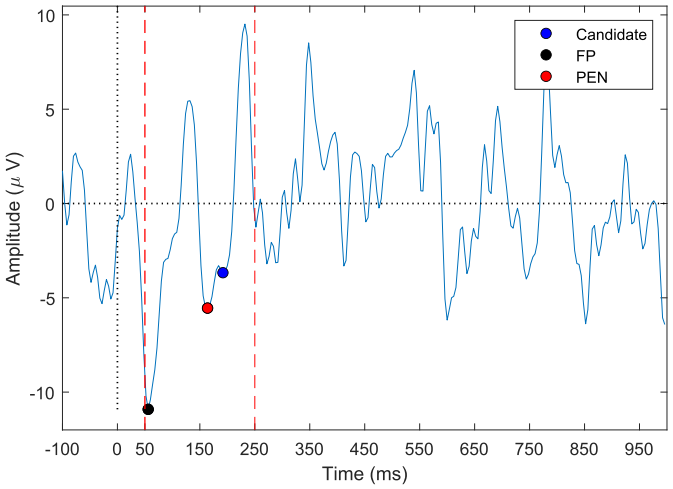

(b)

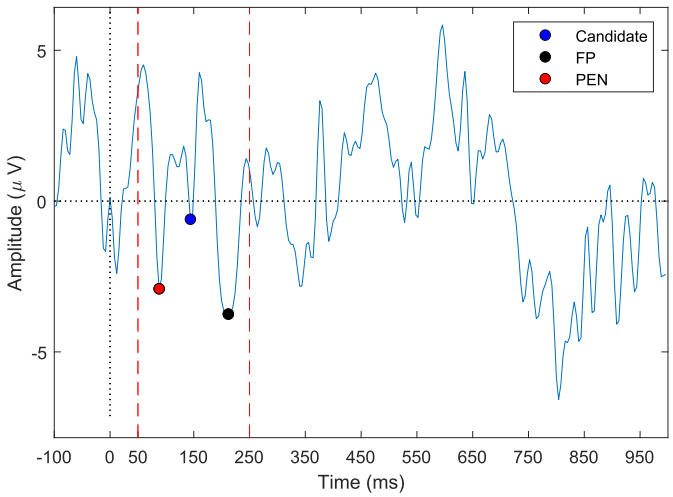

(c)

Fig. 6. Examples of false positives returned by MA, DA, PMA, NCED AA, and CA.

Regarding the performance of the comparative approaches, as the selection mechanism of those is all based on a thresholding manner (DA, AA, MA, PMA, NCED, CA), combining with the similarity to a pre-defined pattern (PMA), or the isolation level (CA), these approaches return false positives when PEN is not the most negative signal in the concerned range as illustrated in Figure 6. Due to the high intra- [27] and inter-subject variability [33], it is challenging to reach an acceptable result with a set of pre-defined parameters. Besides, it has been reported in [12] that the PEN amplitude varied according to the task completion time, which is not well handled by the fixed thresholding mechanism in those approaches. Here, the combination of multiple peak features, in a non-parametric manner has verified the effectiveness of SNCR over the comparative techniques.

V. Conclusion

This paper has introduced a novel EEG peak detection approach in cognitive conflict processing consisting of two stages: multi-scale peak searching and clustering-based ranking. The formal is inherited from an image segmentation technique [30] for candidate calculation, followed by a ranking scheme for PEN determination. Experimental results on a cognitive conflict dataset have verified the advance of SNCR over other EEG and time-series signal processing techniques in terms of accuracy and level of agreement with a neurology expert's selection. The proposed algorithm is developed with a minimized dependence on the parameter used where only the number of time window for the first stage is required. This trait is also essential for the development of promising applications in EEG signal processing, where the intra- and inter-subject variability is not avoidable. As error-related potentials can be exploited to improve the performance of BCIs [10], [40], the dissimilarity between conflict and non-conflict peaks will be investigated in our future work for the enhancement of a communication assistance system.

References

[1] Y. Jia, L. Cui, S. Pollmann, and P. Wei, "The interactive effects of reward expectation and emotional interference on cognitive conflict control: An ERP study," *Physiol. Behav.*, vol. 234, May 2021, Art. no. 113369.

[2] S. Aldini *et al.*, "Effect of mechanical resistance on cognitive conflict in physical human–robot collaboration," in *Proc. Int. Conf. Robot. Autom. (ICRA)*, May 2019, pp. 6137–6143.

[3] A. K. Singh *et al.*, "Visual appearance modulates prediction error in virtual reality," *IEEE Access*, vol. 6, pp. 24617–24624, 2018.

[4] B. Renault, N. Fiori, and S. Giami, "Latencies of event related potentials as a tool for studying motor processing organization," *Biol. Psychol.*, vol. 26, nos. 1–3, pp. 217–230, Jun. 1988.

[5] M. G. H. Coles, G. Gratton, and E. Donchin, "Detecting early communication: Using measures of movement-related potentials to illuminate human information processing," *Biol. Psychol.*, vol. 26, nos. 1–3, pp. 69–89, Jun. 1988.

[6] M. Falkenstein, J. Hohnsbein, J. Hoormann, and L. Blanke, "Effects of crossmodal divided attention on late ERP components. II. Error processing in choice reaction tasks," *Electroencephalogr. Clin. Neurophysiol.*, vol. 78, no. 6, pp. 447–455, 1991.

[7] M. Falkenstein, J. Hohnsbein, J. Hoormann, and L. Blanke, "Effects of errors in choice reaction tasks on the ERP under focused and divided attention," in *Psychophysiological Brain Research*, C. Brunia, A. Gaillard, and A. Kok, Eds. Tilburg, The Netherlands: Tilburg Univ. Press, 1990, pp. 192–195.

[8] W. J. Gehring, B. Goss, M. G. H. Coles, D. E. Meyer, and E. Donchin, "A neural system for error detection and compensation," *Psychol. Sci.*, vol. 4, no. 6, pp. 385–390, 1993.

[9] M. Ullsperger, A. G. Fischer, R. Nigbur, and T. Endrass, "Neural mechanisms and temporal dynamics of performance monitoring," *Trends Cogn. Sci.*, vol. 18, no. 5, pp. 259–267, May 2014.

[10] P. W. Ferrez and J. D. R. Millan, "Error-related EEG potentials generated during simulated brain–computer interaction," *IEEE Trans. Biomed. Eng.*, vol. 55, no. 3, pp. 923–929, Mar. 2008.

[11] O. E. Krigolson and C. B. Holroyd, "Hierarchical error processing: Different errors, different systems," *Brain Res.*, vol. 1155, no. 1, pp. 70–80, 2007.

[12] A. K. Singh, H.-T. Chen, K. Gramann, and C.-T. Lin, "Intraindividual completion time modulates the prediction error negativity in a virtual 3-D object selection task," *IEEE Trans. Cogn. Develop. Syst.*, vol. 12, no. 2, pp. 354–360, Jun. 2020.

[13] A. K. Singh, K. Gramann, H.-T. Chen, and C.-T. Lin, "The impact of hand movement velocity on cognitive conflict processing in a 3D object selection task in virtual reality," *NeuroImage*, vol. 226, Feb. 2021, Art. no. 117578.

[14] D. M. Olvet and G. Hajcak, "The error-related negativity (ERN) and psychopathology: Toward an endophenotype," *Clin. Psychol. Rev.*, vol. 28, no. 8, pp. 1343–1354, 2008.

[15] H. Azami and S. Sanei, "Spike detection approaches for noisy neuronal data: Assessment and comparison," *Neurocomputing*, vol. 133, pp. 491–506, Jun. 2014.

[16] F. E. A. El-Samie, T. N. Alotaiby, M. I. Khalid, S. A. Alshebeili, and S. A. Aldosari, "A review of EEG and MEG epileptic spike detection algorithms," *IEEE Access*, vol. 6, pp. 60673–60688, 2018.

[17] S. Nishida, M. Nakamura, A. Ikeda, and H. Shibasaki, "Signal separation of background EEG and spike by using morphological filter," *Med. Eng. Phys.*, vol. 21, no. 9, pp. 601–608, Nov. 1999.

[18] G. Xu, J. Wang, Q. Zhang, S. Zhang, and J. Zhu, "A spike detection method in EEG based on improved morphological filter," *Comput. Biol. Med.*, vol. 37, no. 11, pp. 1647–1652, Nov. 2007.

[19] S. Li, W. Zhou, Q. Yuan, and Y. Liu, "Seizure prediction using spike rate of intracranial EEG," *IEEE Trans. Neural Syst. Rehabil. Eng.*, vol. 21, no. 6, pp. 880–886, Nov. 2013.

[20] J. Gotman and P. Gloor, "Automatic recognition and quantification of interictal epileptic activity in the human scalp EEG," *Electroencephalogr. Clin. Neurophysiol.*, vol. 41, no. 5, pp. 513–529, Nov. 1976.

[21] J. Zhao and L. Itti, "Classifying time series using local descriptors with hybrid sampling," *IEEE Trans. Knowl. Data Eng.*, vol. 28, no. 3, pp. 623–637, Mar. 2016.

[22] M. Kolodziej, A. Majkowski, R. J. Rak, and A. Rysz, "Detection of spikes with defined parameters in the ECoG signal," *IEEE Trans. Instrum. Meas.*, vol. 68, no. 4, pp. 1045–1052, Apr. 2019.

[23] T.-W. Shen, X. Kuo, and Y.-L. Hsin, "Ant K-means clustering method on epileptic spike detection," in *Proc. 5th Int. Conf. Natural Comput.*, vol. 6, 2009, pp. 334–338.

[24] N. Acır and C. Güzeliş, "Automatic spike detection in EEG by a two-stage procedure based on support vector machines," *Comput. Biol. Med.*, vol. 34, no. 7, pp. 561–575, Oct. 2004.

[25] M. Rácz *et al.*, "Spike detection and sorting with deep learning," *J. Neural Eng.*, vol. 17, no. 1, Jan. 2020, Art. no. 016038.

[26] L. T. Thanh, N. T. A. Dao, N. V. Dung, N. L. Trung, and K. Abed-Meraim, "Multi-channel EEG epileptic spike detection by a new method of tensor decomposition," *J. Neural Eng.*, vol. 17, no. 1, Jan. 2020, Art. no. 016023.

[27] A. Kondacs and M. Szabó, "Long-term intra-individual variability of the background EEG in normals," *Clin. Neurophysiol.*, vol. 110, no. 10, pp. 1708–1716, Oct. 1999.

[28] C.-T. Lin, C.-S. Huang, W.-Y. Yang, A. K. Singh, C.-H. Chuang, and Y.-K. Wang, "Real-time EEG signal enhancement using canonical correlation analysis and Gaussian mixture clustering," *J. Healthcare Eng.*, vol. 2018, pp. 1–11, Jan. 2018.

[29] A. K. Singh and C.-T. Lin, "EnK: Encoding time-information in convolution," 2020, *arXiv:2006.04198*.

[30] T. H. Dinh, M. D. Phung, and Q. P. Ha, "Summit navigator: A novel approach for local maxima extraction," *IEEE Trans. Image Process.*, vol. 29, pp. 551–564, 2020.

[31] F.-A. Savoie, F. Thénault, K. Whittingstall, and P.-M. Bernier, "Visuomotor prediction errors modulate EEG activity over parietal cortex," *Sci. Rep.*, vol. 8, no. 1, pp. 1–16, Dec. 2018.

[32] L. Gehrke *et al.*, "Detecting visuo-haptic mismatches in virtual reality using the prediction error negativity of event-related brain potentials," in *Proc. CHI Conf. Hum. Factors Comput. Syst.*, May 2019, pp. 1–11.

[33] A. Combaz, N. Chumerin, N. V. Manyakov, A. Robben, J. A. K. Suykens, and M. M. Van Hulle, "Error-related potential recorded by EEG in the context of a P300 mind speller brain-computer interface," in *Proc. IEEE Int. Workshop Mach. Learn. Signal Process.*, Aug. 2010, pp. 65–70.

[34] S. Makeig, A. Bell, T.-P. Jung, and T. J. Sejnowski, "Independent component analysis of electroencephalographic data," in *Proc. Adv. Neural Inf. Process. Syst.*, vol. 8, 1995, pp. 1–7.

[35] N. Mtetwa and L. S. Smith, "Smoothing and thresholding in neuronal spike detection," *Neurocomputing*, vol. 69, nos. 10–12, pp. 1366–1370, Jun. 2006.

[36] T. Zhang, R. Ramakrishnan, and M. Livny, "BIRCH: An efficient data clustering method for very large databases," *ACM SIGMOD Rec.*, vol. 25, no. 2, pp. 103–114, Jun. 1996.

[37] M. Ester, H.-P. Kriegel, J. Sander, and X. Xu, "A density-based algorithm for discovering clusters in large spatial databases with noise," in *Proc. KDD*, 1996 vol. 96, no. 34, pp. 226–231.

[38] A. Rodriguez and A. Laio, "Clustering by fast search and find of density peaks," *Science*, vol. 344, no. 6191, pp. 1492–1496, 2014.

[39] J. MacQueen *et al.*, "Some methods for classification and analysis of multivariate observations," in *Proc. 5th Berkeley Symp. Math. Statist. Probab.*, vol. 1, no. 14. Oakland, CA, USA, 1967, pp. 281–297.

[40] F. Iwane, I. Iturrate, R. Chavarriaga, and J. D. R. Millán, "Invariability of EEG error-related potentials during continuous feedback protocols elicited by erroneous actions at predicted or unpredicted states," *J. Neural Eng.*, vol. 18, no. 4, May 2021, Art. no. 046044.